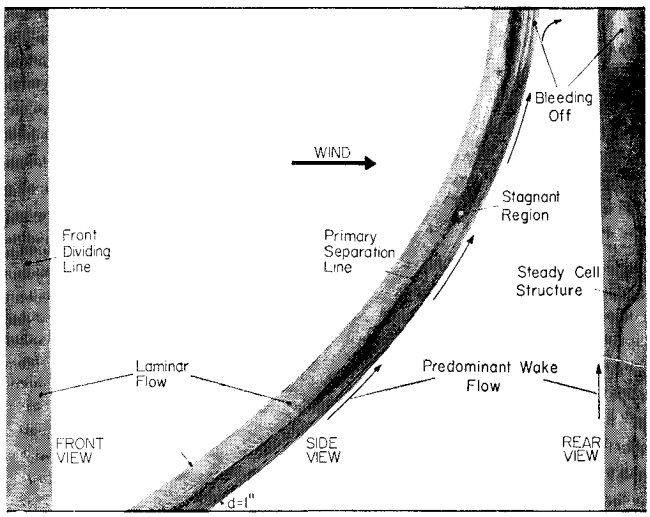

Fig. 3 Three views of the flow pattern around a curved cylinder bowed away from the wind.

3 would indicate that the cylinder was very slightly yawed to the wind, introducing a slight asymmetry in the flow.

Lastly, measurements on flexible curved cylinders (pin-ended at top and bottom in a freestream) gave the local aerodynamic force distribution as a function of ϕ, for various Reynolds numbers and radii of curvature to diameter ratios R/d. Comparison with the prediction for the straight cylinder ($R/d = \infty$), and with the force distribution derived from Fig. 1($R/d = 18$) for the appropriate direction of curvature, shows that the degree of alteration of the wake pressure varies directly with Reynolds number and inversely with R/d (Fig. 5).

The consequence of the poor agreement between the measurement and prediction of the local aerodynamic force on a curved cylinder, is that the cross flow prediction may give a poor estimate of the total drag on such a body. Since the $\sin^2\phi$ relation does not discriminate between directions of curvature, the predicted drag forces are the same for both the curved cylinders tested. This is 21% less than the total drag on a straight cylinder normal to the wind with an equivalent frontal area. However, calculations from the results indicated in Fig. 1 show the drag on the curve away from the wind to be 30% less, whereas that on the curve into the wind is 38% greater. These results are precisely the reverse of the drag forces on hollow half spheres and equivalent circular plates.

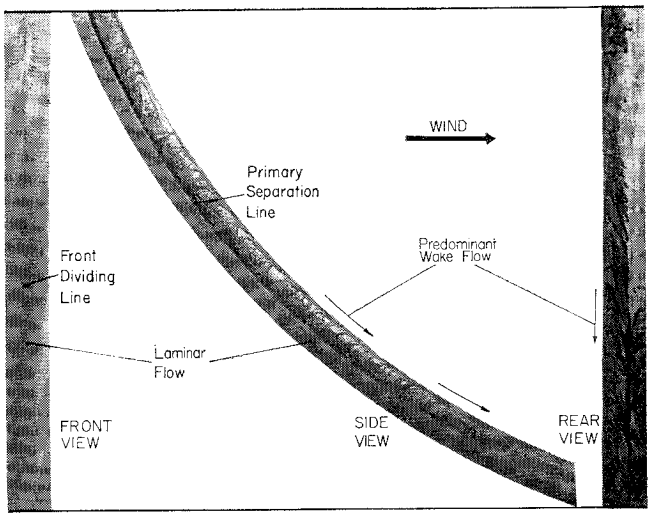

Fig. 4 Three views of the flow pattern around a curved cylinder bowed into the wind.

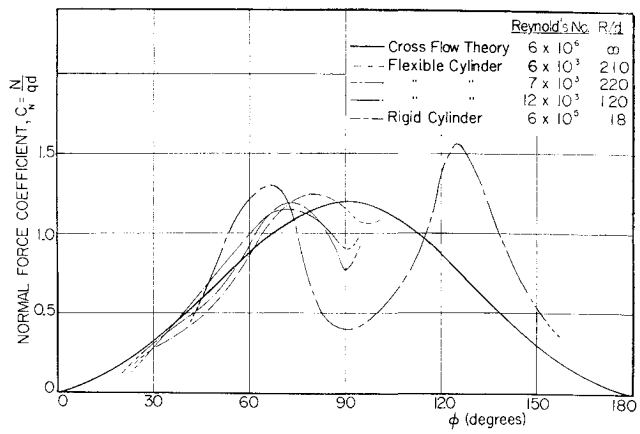

Fig. 5 Normal force coefficient distribution on cylinders curved away from the wind.

It must be concluded that the cross flow relation gives a good description of the flow about curved cylinders, only if the curvature is slight, and that a modification of wake pressures must be considered in estimating the forces on curved cylinders.

References

[1] Surry, J., "Experimental investigation of the characteristics of flow about curved circular cylinders," Insitute for Aerospace Studies, Univ. of Toronto, Toronto, Ontario, Canada, TN 89 (April 1965).

[2] Kuethe, A. M. and Schetzer, J. D., *Foundations of Aerodynamics* (John Wiley & Sons, Inc., New York, 1959).

[3] Rainbird, W. J., Crabbe, R. S., and Jurewicz, L. S., "A water tunnel investigation of the flow separation about circular cones at incidence," National Research Council, Ottawa, Canada, LR-385 (September 1962).

Nomograms for Determining Sonic-Boom Overpressure

Charlie M. Jackson Jr.* and Harry W. Carlson*
NASA Langley Research Center, Hampton, Va.

Nomenclature

C_L = lift coefficient
h = altitude, ft
K_r = reflection constant
l = characteristic length, ft
M = Mach number
P = reference pressure, lb/ft²
P_0 = atmospheric pressure, lb/ft²
ΔP = maximum ground overpressure, lb/ft²
S = wing area, ft²
W = aircraft weight, lb
β = $(M^2 - 1)^{1/2}$

Introduction

THEORETICAL determination of the sonic-boom overpressure of an aircraft in supersonic flight currently involves application of the flight parameters to a set of nondimensional sonic-boom characteristics. These characteristics can be defined by the configuration geometry and the longitudinal lift distribution as described in Ref. 1. The form of the nondimensional characteristics makes the calculation of

Received September 29, 1965; revision received November 5, 1965.

* Aerospace Engineer, Full Scale Research Division.

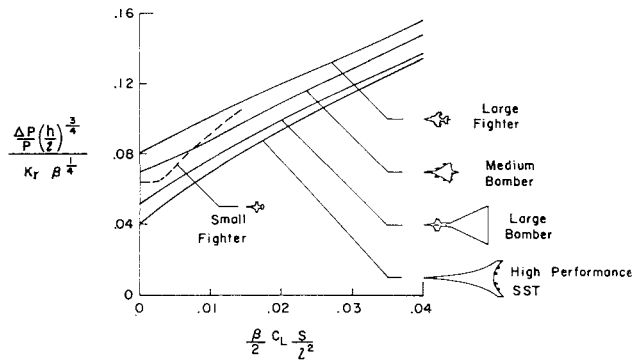

Fig. 1 Representative sonic-boom characteristics of several airplanes.

overpressure for a set of flight conditions (Mach number, altitude, and aircraft weight) quite tedious, and when the aircraft is in a transient phase of flight, such as climb or descent, it is necessary to make these calculations for many sets of flight conditions in order to evaluate the ground overpressure profiles. It is the purpose of this note to present a set of nomograms that allow rapid calculation of maximum ground overpressure for different flight conditions.

Discussion

Sonic-boom characteristics

The currently accepted theory for estimating sonic-boom overpressure for a specific configuration results in expressing the boom in terms of a set of nondimensional characteristics such as those shown in Fig. 1. In Fig. 1 some representative sonic-boom characteristics are shown for several types of aircraft of current interest. These characteristics are for far field conditions and were obtained from a normal distribution of area and equivalent area due to lift. The assumption of far field conditions for the pressure signature (the classical N wave) has been shown to be generally valid for existing airplanes at altitudes normally associated with supersonic flight. As indicated in Ref. 2, future supersonic transports may, because of their extreme length and slenderness, have near-field characteristics which extend to ground level. In that case, the sonic-boom characteristics for a given configuration must be expressed with a family of curves for a set of Mach numbers and distances. The complexity of the characteristic curves is of no concern in the application of the present procedure since this procedure relies only on the form of the nondimensional characteristic coefficients. It should be noted that, although the characteristics of the aircraft presented in Fig. 1 seem to exhibit simple orderly variations with vehicle size, this is not generally the case even for far field characteristics. The inclusion of the small fighter (dashed curve) was made to emphasize this point.

Description and use of nonograms

Nomograms for the calculation of ground overpressure from vehicle characteristics and flight conditions were constructed to be used when the vehicle characteristics are available in the form shown in Fig. 1. These nomograms are presented in

Table 1 Typical lengths and flight weights of aircraft types in Fig. 1

Aircraft type	Typical length, ft	Typical flight wt, lb
Small fighter	50	15,000
Large fighter	70	40,000
Medium bomber	100	90,000
Large bomber	180	400,000
High performance SST	230	350,000

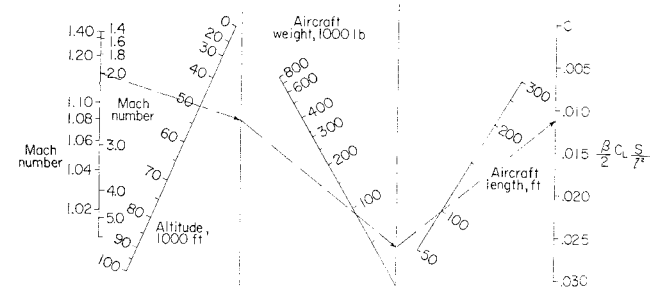

Fig. 2 Nomogram for determining lift parameter from flight conditions.

Figs. 2 and 3. The first nomogram to be used is that of Fig. 2 which converts flight conditions to the lift parameter $(\beta/2) \times C_L(S/l^2)$. The form of this parameter used to construct the nomogram is $[(M^2 - 1)^{1/2}/1.4M^2](W/P_0l^2)$. Because of the nature of the Mach number term (double-valued function) a folded Mach number scale is used on the nomogram. The lift parameter from Fig. 2 is then used to obtain the overpressure parameter from characteristics such as those shown in Fig. 1. The nomogram of Fig. 3 is then used to obtain the overpressure from the overpressure parameter $[(\Delta P/P)(h/l)^{3/4}]/K_r\beta^{1/4}$ and flight conditions. It should be noted that in the construction of the nomograms the reference pressure was defined as the geometric mean of the pressure at flight altitude and sea level. Although more elaborate methods of evaluating the reference pressure are available,[1] the geometric mean is considered sufficient for engineering approximations.

Typical example

In order to compute the ground overpressure using the nomograms of the present method, it is necessary to know the sonic-boom characteristics of the vehicle, flight Mach number, flight altitude, flight weight, and a characteristic length of the vehicle. For convenience, typical lengths and flight weights are given in Table 1 for each of the aircraft types represented in Fig. 1. The data presented in Fig. 1 and Table 1 for the medium bomber are used to present a typical example of the use of the nomograms of Figs. 2 and 3. For flight conditions at a Mach number of 2.0 and altitude of 50,000 ft, the necessary operations are outlined on the nomograph of Fig. 2 (dashed lines) to obtain a value of the lift parameter $(\beta/2)C_L(S/l^2)$ of 0.0112. With this value of the lift parameter and the characteristic curve for the medium bomber (Fig. 1) the overpressure parameter $[(\Delta P/P)(h/l)^{3/4}]/K_r\beta^{1/4}$ is determined to be 0.09. The nomogram of Fig. 3 is now used with the overpressure parameter, the flight conditions, and a reflection constant K_r of 1.9 (a suggested value for average ground conditions). The necessary operations are outlined on Fig. 3 (dashed lines), and the resulting maximum ground overpressure is 1.32 psf.

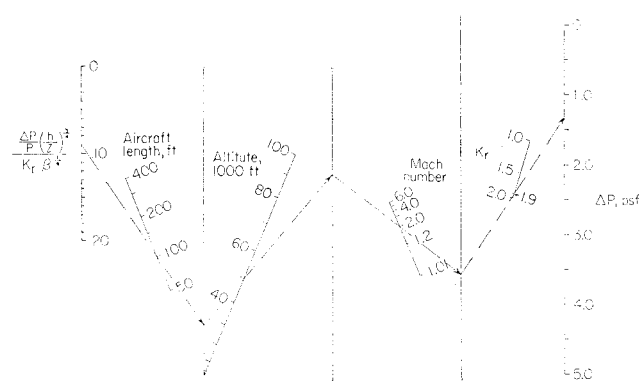

Fig. 3 Nomogram for determining maximum ground overpressure from overpressure parameter and flight conditions.

References

[1] Carlson, H. W., "Correlation of sonic-boom theory with wind-tunnel and flight measurements," NASA TR R-213 (December 1964).

[2] Carlson, H. W., McLean, F. E., and Middleton, W. D., "Prediction of airplane sonic-boom pressure fields," NASA Conference on Aircraft Operating Problems, NASA SP-83, pp. 235–244(1965).

Chordwise Divergence of Rectangular Flat Plate Wings at Supersonic Speeds

A. J. Rhodes*
British Aircraft Corporation, Bristol, England

AND

D. J. Johns†
Loughborough College of Technology, Loughborough, England

Nomenclature

a	=	speed of sound
A_E	=	aeroelastic lift efficiency
C	=	wing chord
C_{mn}, d_n	=	generalized coordinates
E	=	Young's modulus
$f(\vartheta)$, $F(\vartheta)$	=	spanwise mode shapes
$g(\eta)$, $G(\eta)$	=	chordwise mode shapes
l	=	wing span (root to tip)
L_j	=	lift/unit incidence of element j
m, n	=	integers
M	=	Mach number
r_m	=	generalized coordinates
t	=	wing thickness
W	=	wing deflection
α	=	incidence of rigid wing
α_j	=	change in incidence, due to deformation, of element j
β	=	$(M^2 - 1)^{1/2}$
η	=	nondimensional chordwise coordinate
ζ	=	nondimensional spanwise coordinate
ρ	=	air density
$\varphi(\zeta,\eta)$	=	deflection function

Introduction

In most of the published papers dealing with the chordwise divergence of rectangular flat plate wings clamped along their root chord it has been assumed that the spanwise mode shape is relatively unimportant, compared with the chordwise mode shape, and can be fixed arbitrarily. The wide variation in the results obtained (Fig. 1) has shown the need for analyses not embodying this assumption. Such analyses have been made by Rhodes[1] using completely general assumed deflection modes and Ackeret aerodynamic theory.

Previous studies using Ackeret aerodynamic theory have been made by Biot,[2,3] Broadbent[4] and Martin.[5] For a two-dimensional wing with no spanwise bending, Biot[2] derived an exact stability criterion for chordwise divergence which may be written

$$(E/\rho a^2)(t/l)^3 > 0.43(C/l)^3 M^2/\beta \qquad (1)$$

The stabilizing influence of the anticlastic curvature induced by spanwise bending was shown in later papers by Biot,[2,3] and the influence of the assumed spanwise mode on the results was also indicated. Thus, if

$$W = f_{(\zeta)} \cdot g_{(\eta)} = \zeta^2(3 - \zeta) \sum_{n=0}^{6} d_n \eta^n \qquad (2)$$

divergence was not possible for flat plates of aspect ratio 3 and 1.5.

More recent studies by the authors using as modes

$$\left.\begin{aligned} W &= \zeta^2(3 - \zeta) \sum_{n=0}^{2} d_n \eta^n + \zeta(2 - \zeta) \sum_{m=1}^{2} r_m \eta^m \\ \text{i. e.} \quad W &= f_{(\zeta)} \cdot g_{(\eta)} + F_{(\zeta)} G_{(\eta)} \end{aligned}\right\} \qquad (3)$$

showed that divergence was possible at least for aspect ratios up to 2 (Fig. 1). Note that function $F \cdot G$ only satisfies the condition $\partial W/\partial\zeta = 0$ at $\eta = 0$.

Also shown in Fig. 1 are results using the modes

$$W = d_1\zeta^3\eta^2 + d_2\zeta^2\eta \qquad (4)$$

as well as those from Refs. 1–5.

Broadbent[4] assumed that the plate deformed in a cylindrical mode about a generator through the root leading edge swept at 45° to the freestream. He obtained the following stability criterion:

$$(E/\rho a^2)(t/l)^3 > 0.3M^2/\beta \qquad (5)$$

Martin[5] assumed

$$W = (d_1 + d_2)\zeta^3\eta^2 + d_3[(\zeta^2/2) - (\zeta^3/3) + (\zeta^4/12)] + d_4\eta(2\zeta - \zeta^2) \qquad (6)$$

where d_1 and d_2 are generalized coordinates for chordwise deformation forward of, and aft of, the mid chord, respectively. The results indicated that divergence was possible for low aspect ratio plate wings at high supersonic speeds.

Hancock[6] used an approximate, linearized, supersonic pressure distribution, which is much more general than Ackeret theory, and compared his results with Ref. 7, which used linearized slender wing theory and is only valid for low aspect ratios at $M \doteq 1$. Hancock showed, using as assumed modes

$$W = \tfrac{1}{26}(45\zeta^2 - 20\zeta^3 + \zeta^6)g_{(\eta)} \qquad (7)$$

that chordwise divergence was not possible outside of the

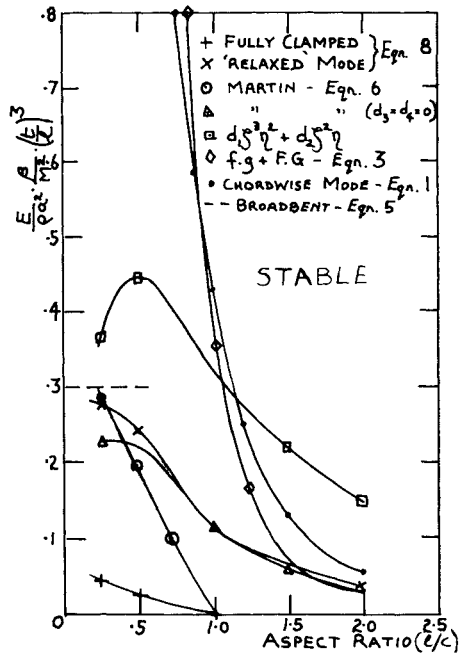

Fig. 1 Flat plate stability boundaries for $M \gg 1$.

Received February 10, 1965; revision received August 19, 1965.

* Technical Officer.

† Reader in Aeronautical Engineering.